

Squeezed States of Light for Future Gravitational Wave Detectors at a Wavelength of 1550 nm

Fabian Meylahn¹,* Benno Willke², and Henning Vahlbruch²

Max Planck Institute for Gravitational Physics (Albert Einstein Institute), D-30167 Hannover, Germany and Leibniz Universität Hannover, D-30167 Hannover, Germany

 (Received 29 June 2022; accepted 26 August 2022; published 16 September 2022)

The generation of strongly squeezed vacuum states of light is a key technology for future ground-based gravitational wave detectors (GWDs) to reach sensitivities beyond their quantum noise limit. For some proposed observatory designs, an operating laser wavelength of 1550 nm or around $2\ \mu\text{m}$ is required to enable the use of cryogenically cooled silicon test masses for thermal noise reduction. Here, we present for the first time the direct measurement of up to 11.5 dB squeezing at 1550 nm over the complete detection bandwidth of future ground-based GWDs ranging from 10 kHz down to below 1 Hz. Furthermore, we directly observe a quantum shot-noise reduction of up to (13.5 ± 0.1) dB at megahertz frequencies. This allows us to derive a precise constraint on the absolute quantum efficiency of the photodiode used for balanced homodyne detection. These results hold important insight regarding the quantum noise reduction efficiency in future GWDs, as well as for quantum information and cryptography, where low decoherence of nonclassical states of light is also of high relevance.

DOI: [10.1103/PhysRevLett.129.121103](https://doi.org/10.1103/PhysRevLett.129.121103)

Since the first detection of gravitational waves in 2015 [1], a network of ground-based gravitational wave detectors (GWDs) [2] has opened a new view into our Universe [3]. In the last gravitational wave observation run (O3) the advanced LIGO [4,5], advanced Virgo [6], and GEO600 [7] detectors used squeezed states (SQZ) of light to extend their astrophysical reach. The LIGO and Virgo detectors reached a shot-noise reduction of about 3 dB [8,9], and at GEO600 recently a quantum shot-noise reduction of 6 dB was demonstrated [10]. The quantum noise limitation of GWDs is composed of the shot noise at higher detection frequencies and the quantum radiation pressure noise at lower frequencies. For a quantum noise reduction over the full detection band, the frequency-independent squeezed light can be converted into frequency-dependent states with optical filter cavities [11]. This was demonstrated at GWD detection frequencies [12,13], and intense research activities for integration at the advanced detectors are ongoing.

Two design concepts of the optical parametric amplifier (OPA), which generates the squeezed states via the process of parametric down-conversion, are implemented in the current GWDs operating at a laser wavelength of 1064 nm. Linear, half monolithic OPA cavities are used at GEO600

and Virgo [14,15]. With this kind of OPA the highest squeezing factors have been demonstrated: 15 dB in the megahertz range [16] and 12.0 dB in the audio band [17], the latter of which is relevant for current GWDs. The LIGO GWDs use a bowtie OPA design [18,19]. One important difference between the two OPA topologies is that the bowtie configuration is less sensitive to backscattered light because of the two distinct traveling wave directions inside the cavity. This leads to an intrinsic suppression, comparable to a conventional Faraday isolator, but without introducing additional optical loss [18]. In a separate experiment 11.6 dB squeezed light in the audio band was demonstrated using this OPA design [20].

The application of squeezed light is a key technology in the design of all next generation GWDs, demanding an effective quantum noise reduction of 10 dB in the gravitational wave detection channel [21,22]. Some of the future GWDs aim to reduce mirror thermal noise via cryogenic cooling combined with appropriate mirror materials like silicon. This requires a change in the operating wavelength from 1064 to 1550 nm or $2\ \mu\text{m}$ [21–23] and the development of high-efficiency squeezed light sources at these wavelengths. So far, squeezing levels of 13.1 dB [24] and 7.2 dB [25] have been demonstrated in the megahertz regime at 1550 and 2128 nm, respectively. At audio-band frequencies, 11.4 dB [26] and 4 dB [27] were achieved at 1550 and 1984 nm without the stabilization of the squeezed light phase. With a phase stabilization, 8.2 dB [28] and 3.9 dB [29] were reported. None of the demonstrated squeezed light sources was able to generate and detect

Published by the American Physical Society under the terms of the Creative Commons Attribution 4.0 International license. Further distribution of this work must maintain attribution to the author(s) and the published article's title, journal citation, and DOI. Open access publication funded by the Max Planck Society.

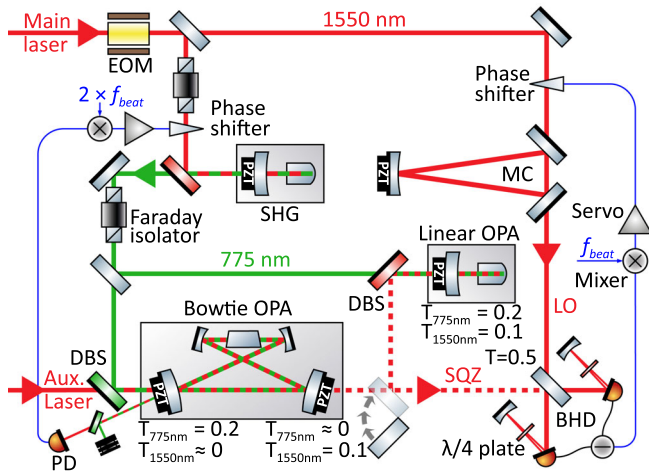


FIG. 1. Simplified schematic of the experimental setup.

squeezed states of light in the most relevant detection band for future GWDs below a frequency of 500 Hz.

Here we present the first efficient generation and the detection of squeezed light down to 0.5 Hz at a wavelength of 1550 nm using a bowtie style OPA cavity. For a precise characterization, we compare the bowtie with a linear OPA cavity at megahertz frequencies by evaluating models for the optical loss and phase noise of the squeezed fields. Thereby, we can also characterize the quantum efficiency of the used positive-intrinsic-negative (*p-i-n*) photodiodes (PDs) as well as the internal losses of the OPAs. All these contributions to the loss and phase noise budget limit the maximum achievable quantum noise reduction via squeezed states of light and therefore a high PD quantum efficiency is required by GWDs.

A simplified sketch of the experimental setup is shown in Fig. 1. The main laser source is stabilized in power and frequency and is described in detail in Ref. [30]. Approximately 310 mW of the laser's output power are split off and serve as the main laser input field (Main laser) for the squeezing setup. Via an electro-optical modulator (EOM), which is driven at a frequency of 115 MHz, a phase modulation is imprinted on the light field. This enables the length stabilization of four optical cavities to establish the resonance condition for their input laser fields via the Pound-Drever-Hall sensing scheme [31]. The feedback signals of the individual control loops are sent to the cavities' piezoelectric length control elements (PZTs). For simplicity, the control loops of the cavities are omitted in Fig. 1.

A fraction of the main laser beam is injected into the second harmonic generator (SHG) where the pump beam for the OPAs downstream is generated. Another part of the 1550 nm main beam is used as a local oscillator (LO) for the balanced homodyne detection (BHD), after it passes a triangular mode cleaner cavity (MC) providing a spatially filtered beam with insignificant low astigmatism [32].

For BHD, the LO is spatially overlapped with the signal field. The signal field's amplitude is read out along the quadrature defined by the phase of the LO phase [20].

We found that about 0.5% of the incident light is reflected from the BHD PDs. These *p-i-n* InGaAs PDs have an antireflection (AR) coated sensor of 2 mm diameter, the commonly used size in GWDs [33], and two curved mirrors serve as retroreflectors to recycle the reflected light for a higher effective PD quantum efficiency. Additionally, quarter wave plates are placed in front of the retroreflectors, thereby rotating the recycled light into the orthogonal polarization. In this way, the interference of residual back-reflections from the homodyne detector toward the OPA cavities in the polarization of the squeezed light are suppressed and less (phase) noise is added (see Ref. [34], p. 43).

Our experimental setup contains two different OPAs, which are constructed in a linear and bowtie configuration, respectively. As shown in Fig. 1, a movable mirror in the signal input port of the BHD can be used to select which of the OPA output fields is sent toward the BHD. Common to both OPAs is that they are designed to be double resonant for 1550 and 775 nm, respectively. The 775 nm pump field is used to stabilize the cavities on resonance, whereas the (anti)squeezing is produced at 1550 nm. A segmented heating scheme of the nonlinear crystal ensures good quasi-phase-matching of the corresponding fields for an efficient squeezed light generation and simultaneous resonance of both fields [15,28].

In a first step, to determine the homodyne detector PD quantum efficiency we employed the linear OPA and determined all relevant parameters. Our hemilithic linear OPA cavity contains a periodically poled potassium titanyl phosphate (PPKTP) crystal with the dimensions $1.0 \times 2.0 \times 11.5$ mm. The highly reflective, curved crystal face serves as the cavity end mirror, while the plane face has an antireflective coating. A partly transmissive mirror is used for the pump light in-coupling and the squeezed light out-coupling. The generated squeezed states are separated from the pump field via a dichroic beam splitter (DBS) and sent toward the BHD.

For three different OPA pump powers the corresponding quantum noise variances are measured at the output of the BHD and presented in reference to the vacuum noise in Fig. 2. With a pump power of 19 mW, a maximum quantum noise reduction of up to (13.5 ± 0.1) dB is measured, which is the highest demonstrated vacuum noise reduction at this wavelength to date. Taking also the measurements with lower pump powers into account, we derived a consistent model which describes the optical loss and phase noise for the corresponding (anti)squeezing [16]. For all the measurements shown in Fig. 2, this model implies a total detection efficiency of $(96.5 \pm 0.2)\%$ and (5 ± 1) mrad phase noise.

We can now break down the overall detection efficiency into the known individual contributions. First, the

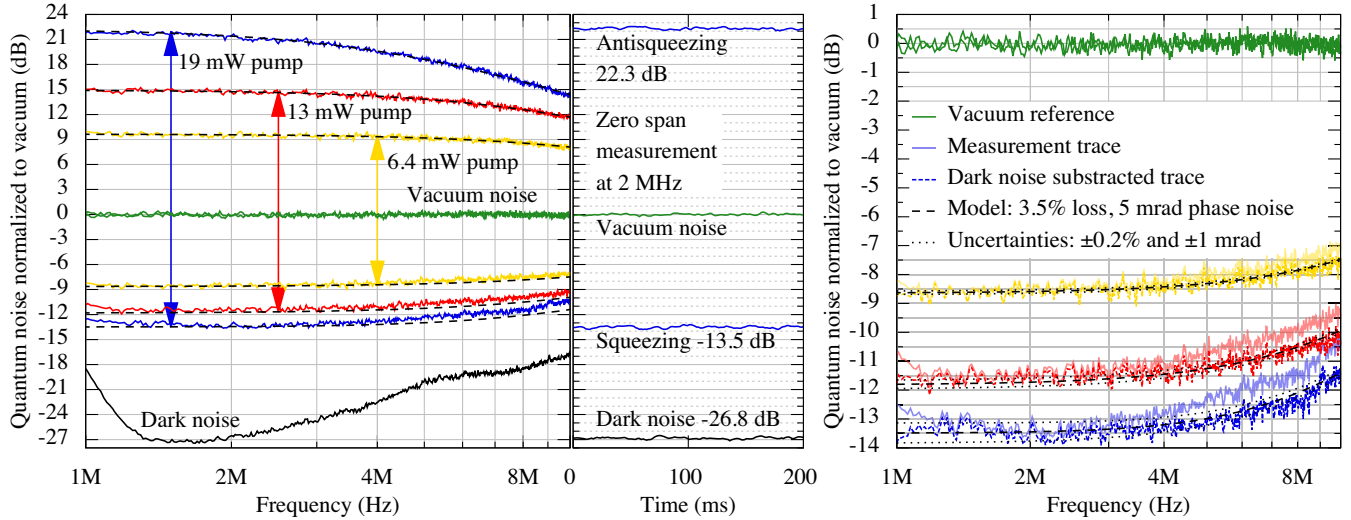


FIG. 2. Homodyne measurements with the signal input from the linear OPA. Left: noise spectra of the (anti)squeezing using three different OPA pump powers normalized to the vacuum noise reference for 20 mW local oscillator power at frequencies between 1 and 10 MHz. The measurements were modeled to estimate the optical loss and phase noise for the squeezed states. The best fits (see black dashed curves) were obtained with an optical loss of $(3.5 \pm 0.2)\%$ and a phase noise of (5 ± 1) mrad. All spectra are captured with a resolution bandwidth (RBW) of 300 kHz and a video bandwidth (VBW) of 100 Hz (left and right). Center: a zero span measurement at 2 MHz over 200 ms time confirms the detection of (13.5 ± 0.1) dB squeezing (RBW 100 kHz, VBW 30 Hz). Right: enlargement of the measured quantum noise reduction of the left-hand graph. The uncertainties of our model fits are illustrated with dotted black lines.

homodyne contrast was measured to $(99.5 \pm 0.05)\%$, which corresponds to an optical loss of $(1.0 \pm 0.1)\%$. Second, we determined the transmission loss through three lenses and the antireflection coating of the beam splitter back side to $(0.05 \pm 0.02)\%$ in an independent measurement. Third, we calculated the OPA escape efficiency to be $(99.0 \pm 0.4)\%$ based on our measurements of the free spectral range (FSR) (3443.0 ± 0.2) MHz, the cavity full width at half maximum frequency (FWHM) (59.2 ± 0.2) MHz, and the transmission of the coupling mirror $(10.15 \pm 0.02)\%$ at a wavelength of 1550 nm. The FSR and FWHM were measured with a bright laser beam at 1550 nm wavelength with strong phase modulation sidebands imprinted for calibration. The power transmission of the coupling mirror was measured with a power stabilized laser. Furthermore, we characterized in an independent measurement the highly reflective (HR) coating of the PPKTP crystal by determining the reduction of the reflected power at 1550 nm of the light, which is coupled into the OPA via the back side of the crystal, when the OPA is on resonance. The measured depletion of $(1.25 \pm 0.13)\%$ implies a residual transmission of the HR coating of (340 ± 40) ppm. To explain the escape efficiency, (280 ± 180) ppm single path loss through the PPKTP crystal remains, which includes the absorption in the crystal, scattering, and reflection of the AR coating of the crystal.

From all these measurements one can conclude that, in order to be in agreement with the model parameters as derived from the measurements shown in Fig. 2, the absolute quantum efficiency of the homodyne detector

PDs has to be $(98.5 \pm 0.7)\%$ including the enhancement in sensitivity of 0.5% gained with the retroreflectors.

Based on the precise characterization of the detection efficiency and given the above loss estimation for the PPKTP crystal material, we can now study the bowtie OPA in more detail. This OPA design aimed for minimal astigmatism of the squeezed field mode in order to obtain a high contrast with any nonastigmatic Gaussian beam as it is used, e.g., for the BHD local oscillator beam or in GWDs. To this end, two concave mirrors ($r = -100$ mm) focus the beam into the double-sided 0.5° wedged and AR coated 11.5-mm-long PPKTP crystal. The focus radius inside the crystal is $47 \mu\text{m}$, which requires a higher pump power compared to the linear cavity, where the waist size is $40 \mu\text{m}$ in radius. The two coupling mirrors are convex, $r = +1000$ mm, to reduce astigmatism, which is introduced by the bowtie geometry and spherical curved mirrors, and to provide an OPA output field with a low beam divergence. All cavity mirrors are clamped under 5° angle of incidence on a rigid aluminum spacer with one PZT per coupling mirror for cavity length actuation, as shown in Fig. 1.

A BHD contrast measurement of $(99.85 \pm 0.05)\%$ experimentally confirms the low level of astigmatism: a squeezing detection loss of only $(0.3 \pm 0.1)\%$ is introduced by the nonperfect mode overlap at this stage. Similar to the linear OPA, we determined the bowtie OPA escape efficiency to $(98.7 \pm 0.6)\%$, calculated from individual measurements of the FSR (464.74 ± 0.04) MHz, the FWHM (8.14 ± 0.04) MHz, and the 1550 nm coupler transmission

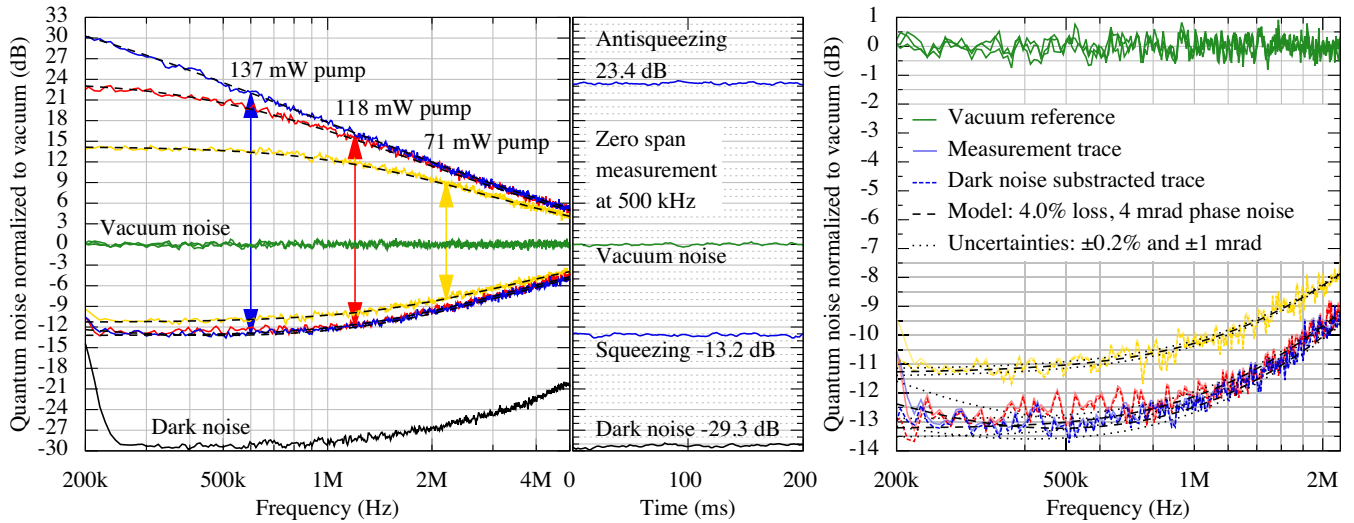


FIG. 3. Homodyne measurements with the signal input from the bowtie OPA. Left: noise spectra of the (anti)squeezing using three different OPA pump powers normalized to the vacuum noise reference for 20 mW local oscillator power at frequencies between 200 kHz and 5 MHz. Given the high electronic dark noise clearance a noise subtraction has only minor impact on the model (black dashed curves), which was found to fit best with $(4.0 \pm 0.2)\%$ optical loss and (4 ± 1) mrad phase noise. All spectra are captured with a RBW 100 kHz and VBW 100 Hz (left and right). Center: zero span measurement at 500 kHz over 200 ms time confirms the detection of (13.2 ± 0.1) dB squeezing (RBW 50 kHz, VBW 30 Hz). Right: enlargement of the measured quantum noise reduction of the left-hand graph. The uncertainties of our model fit are illustrated with the dotted black lines.

of $(10.303 \pm 0.012)\%$. Compared to the linear OPA, the bowtie OPA shows a slightly lower escape efficiency. This can be explained by the higher transmission of the 775 nm coupling mirror at 1550 nm wavelength of (3340 ± 120) ppm. With the above estimation of the homodyne detector PD quantum efficiency, the total optical loss budget for the bowtie squeezing path adds up to $(3.1 \pm 1.4)\%$, which is in agreement with the expected optical loss taken from the fits of the measurements as presented in Fig. 3 of $(4.0 \pm 0.2)\%$. The highest squeezing level we could measure with the bowtie OPA is (13.2 ± 0.1) dB at a harmonic pump power of 137 mW and is thus comparable in squeezing strength to the results we achieved with the linear OPA.

In contrast to the relatively short measurement times required at megahertz frequencies, where no active phase control scheme was necessary to capture the presented measurements, the phase of the (anti)squeezed state has to be stabilized to the readout quadrature of the BHD to demonstrate the performance below 10 kHz. Following the coherent control scheme [35], we therefore injected a frequency shifted auxiliary control field into the bowtie OPA. A beat signal between the auxiliary laser field and the main laser field is used for an offset phase lock loop (PLL) that stabilize the laser frequency difference to 7.15 MHz (not shown in Fig. 1). This optical beat frequency readout f_{beat} also serves as the electronic local oscillator input source for the error signal generation required for phase stabilization, which circumvents a very high bandwidth PLL. The beat frequency is doubled with an electronic mixer for the pump phase error signal generation.

In this configuration we performed squeezing measurements from 10 kHz down to below 1 Hz, and the noise spectra are shown in Fig. 4. Each trace is computed from a 120-s-long time series, sampled with 22 kS/s. The averaging factor varies between 38 for frequencies below 1.7 Hz and 377 000 for the frequencies between 1.7 kHz and 10 kHz. The measurement time was limited

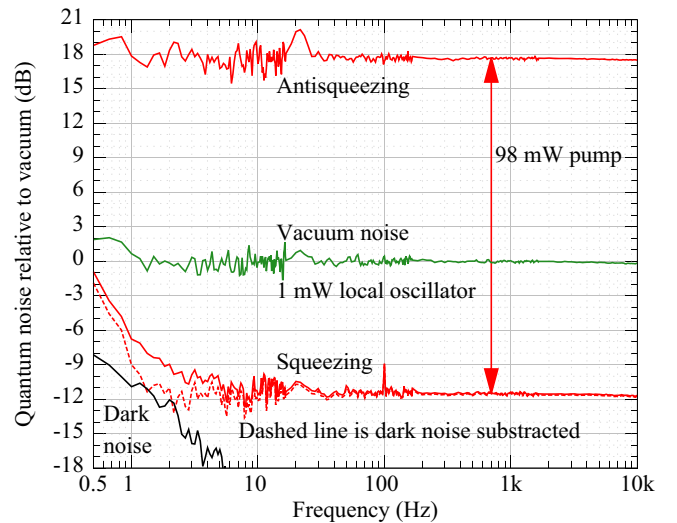


FIG. 4. Quantum noise measurements from 10 kHz down to 0.5 Hz obtained with the bowtie OPA. The results correspond to a harmonic OPA pump power of 98 mW and are plotted relative to the vacuum noise reference. The dashed curve illustrates the squeezing level after the electronic dark noise was subtracted.

to about 120 s due to noise transients, occurring approximately every few 100 s. We suspect that single dust particles, passing the beam in one arm of the BHD, might be the origin of these events [20]. Time traces with at least one of these events lead to noise spectra with a noise shoulder below a few 10 Hz.

Nevertheless, a quantum noise reduction of up to 11.5 dB is detected at audio-band frequencies with as little as 17.5 dB antisqueezing. Below a few hertz the residual electronic dark noise contribution limits the direct squeezing measurement, but the dark noise subtraction reveals the full potential of our squeezed light source, leading to a squeezing level of 9 dB at 1 Hz frequency.

At these low measurement frequencies we observed several increased noise couplings in the squeezing setup. For example, the laser power noise shows up at the homodyne detector stage below 2 Hz, probably due to air flow and particles passing the beams. For the measurements we show here, we therefore optimized the local oscillator power and carefully checked the linearity of the BHD. Above 2 Hz the measurement is mostly limited by the technical noise of the coherent control field beating with the local oscillator field. This white noise source is at about -18 dB relative to the vacuum noise and led to about 0.5 dB squeezing degradation.

In conclusion, we reported on the first demonstration of strongly squeezed vacuum states of light at a wavelength of 1550 nm at detection frequencies spanning the complete range of current [4,6,7,36] and future ground-based GWDs [21,37]. We measured squeezing at frequencies from 10 kHz down to 0.5 Hz with a quantum noise reduction of up to 11.5 dB, which highlights the potential of the proposed quantum noise reduction schemes for future GWDs with silicon test masses, e.g., the low frequency interferometers of the Einstein Telescope GWD [21]. Without the special technical difficulties for squeezing measurements that arise from the long measurement time in the audio band, we were able to demonstrate more than 13 dB quantum noise reduction at megahertz frequencies, for both the linear and the bowtie OPA configuration. However, the bowtie design might be beneficial for the application in GWDs as the intrinsic immunity to back-scattering [18,20], but requires further optimization of the cavity mirror coatings to reach an escape efficiency as high as the one we achieved with the linear OPA. Finally, we demonstrated that a careful design of the bowtie cavity geometry allows for very low astigmatism competitive to linear designs. The gained knowledge on the 2 mm photodiode quantum efficiency, the optical loss of current PPKTP crystal material, and the investigation of limitations for the audio-band and sub-audio-band squeezing pave the way for the design of squeezed light sources and photodetectors for future GWDs operating at 1550 nm.

This work was funded by the Deutsche Forschungsgemeinschaft (DFG, German Research Foundation) under Germany's Excellence Strategy–EXC-2123 Quantum Frontiers–390837967.

- *fabian.meylahn@aei.mpg.de
- [1] B. P. Abbott *et al.* (LIGO Scientific Collaboration and Virgo Collaboration), Observation of Gravitational Waves from a Binary Black Hole Merger, *Phys. Rev. Lett.* **116**, 061102 (2016).
 - [2] B. P. Abbott *et al.* (KAGRA, LIGO Scientific, and Virgo Collaborations), Prospects for observing and localizing gravitational-wave transients with Advanced LIGO, Advanced Virgo and KAGRA, *Living Rev. Relativity* **23**, 3 (2020).
 - [3] R. Abbott *et al.* (LIGO Scientific Collaboration, Virgo Collaboration, and KAGRA Collaboration), GWTC-3: Compact binary coalescences observed by LIGO and Virgo during the second part of the third observing run, *arXiv: 2111.03606*.
 - [4] J. Aasi *et al.* (LIGO Scientific Collaboration), Advanced LIGO, *Classical Quantum Gravity* **32**, 074001 (2015).
 - [5] A. Buikema *et al.*, Sensitivity and performance of the Advanced LIGO detectors in the third observing run, *Phys. Rev. D* **102**, 062003 (2020).
 - [6] F. Acernese *et al.* (Virgo Collaboration), Advanced Virgo: A second-generation interferometric gravitational wave detector, *Classical Quantum Gravity* **32**, 024001 (2015).
 - [7] K. L. Dooley *et al.*, GEO 600 and the GEO-HF upgrade program: Successes and challenges, *Classical Quantum Gravity* **33**, 075009 (2016).
 - [8] F. Acernese *et al.* (Virgo Collaboration), Increasing the Astrophysical Reach of the Advanced Virgo Detector via the Application of Squeezed Vacuum States of Light, *Phys. Rev. Lett.* **123**, 231108 (2019).
 - [9] M. Tse *et al.*, Quantum-Enhanced Advanced LIGO Detectors in the Era of Gravitational-Wave Astronomy, *Phys. Rev. Lett.* **123**, 231107 (2019).
 - [10] J. Lough, E. Schreiber, F. Bergamin, H. Grote, M. Mehmet, H. Vahlbruch, C. Affeldt, M. Brinkmann, A. Bisht, V. Kringel, H. Lück, N. Mukund, S. Nadji, B. Sorazu, K. Strain, M. Weinert, and K. Danzmann, First Demonstration of 6 dB Quantum Noise Reduction in a Kilometer Scale Gravitational Wave Observatory, *Phys. Rev. Lett.* **126**, 041102 (2021).
 - [11] H. J. Kimble, Y. Levin, A. B. Matsko, K. S. Thorne, and S. P. Vyatchanin, Conversion of conventional gravitational-wave interferometers into quantum nondemolition interferometers by modifying their input and/or output optics, *Phys. Rev. D* **65**, 022002 (2001).
 - [12] Y. Zhao *et al.*, Frequency-Dependent Squeezed Vacuum Source for Broadband Quantum Noise Reduction in Advanced Gravitational-Wave Detectors, *Phys. Rev. Lett.* **124**, 171101 (2020).
 - [13] L. McCuller, C. Whittle, D. Ganapathy, K. Komori, M. Tse, A. Fernandez-Galiana, L. Barsotti, P. Fritschel, M. MacInnis, F. Matichard, K. Mason, N. Mavalvala, R. Mittleman, H. Yu, M. E. Zucker, and M. Evans, Frequency-Dependent Squeezing for Advanced LIGO, *Phys. Rev. Lett.* **124**, 171102 (2020).
 - [14] J. Abadie *et al.* (The LIGO Scientific Collaboration), A gravitational wave observatory operating beyond the quantum shot-noise limit, *Nat. Phys.* **7**, 962 (2011).

- [15] M. Mehmet and H. Vahlbruch, The squeezed light source for the Advanced Virgo detector in the observation run O3, *Galaxies* **8**, 79 (2020).
- [16] H. Vahlbruch, M. Mehmet, K. Danzmann, and R. Schnabel, Detection of 15 dB Squeezed States of Light and their Application for the Absolute Calibration of Photoelectric Quantum Efficiency, *Phys. Rev. Lett.* **117**, 110801 (2016).
- [17] M. Mehmet and H. Vahlbruch, High-efficiency squeezed light generation for gravitational wave detectors, *Classical Quantum Gravity* **36**, 015014 (2018).
- [18] S. S. Y. Chua, M. S. Stefszky, C. M. Mow-Lowry, B. C. Buchler, S. Dwyer, D. A. Shaddock, P. K. Lam, and D. E. McClelland, Backscatter tolerant squeezed light source for advanced gravitational-wave detectors, *Opt. Lett.* **36**, 4680 (2011).
- [19] A. R. Wade, G. L. Mansell, S. S. Y. Chua, R. L. Ward, B. J. J. Slagmolen, D. A. Shaddock, and D. E. McClelland, A squeezed light source operated under high vacuum, *Sci. Rep.* **5**, 18052 (2015).
- [20] M. S. Stefszky, C. M. Mow-Lowry, S. S. Y. Chua, D. A. Shaddock, B. C. Buchler, H. Vahlbruch, A. Khalaidovski, R. Schnabel, P. K. Lam, and D. E. McClelland, Balanced homodyne detection of optical quantum states at audio-band frequencies and below, *Classical Quantum Gravity* **29**, 145015 (2012).
- [21] ET Steering Committee, Einstein gravitational wave Telescope, Technical Report No. ET-0007B-20, 2020, <https://apps.et-gw.eu/tds/ql/?c=15418>.
- [22] D. Reitze *et al.*, Cosmic explorer: The U.S. contribution to gravitational-wave astronomy beyond LIGO, *Bull. Am. Astron. Soc.* **51**, 035 (2019), <https://baas.aas.org/pub/2020n7i035>.
- [23] M. Evans *et al.*, A horizon study for cosmic explorer: Science, observatories, and community, [arXiv:2109.09882](https://arxiv.org/abs/2109.09882).
- [24] A. Schönbeck, F. Thies, and R. Schnabel, 13 dB squeezed vacuum states at 1550 nm from 12 mW external pump power at 775 nm, *Opt. Lett.* **43**, 110 (2018).
- [25] C. Darsow-Fromm, J. Gurs, R. Schnabel, and S. Steinlechner, Squeezed light at 2128 nm for future gravitational-wave observatories, *Opt. Lett.* **46**, 5850 (2021).
- [26] M. Mehmet, S. Ast, T. Eberle, S. Steinlechner, H. Vahlbruch, and R. Schnabel, Squeezed light at 1550 nm with a quantum noise reduction of 12.3 dB, *Opt. Express* **19**, 25763 (2011).
- [27] G. L. Mansell, T. G. McRae, P. A. Altin, M. J. Yap, R. L. Ward, B. J. J. Slagmolen, D. A. Shaddock, and D. E. McClelland, Observation of Squeezed Light in the 2 μm Region, *Phys. Rev. Lett.* **120**, 203603 (2018).
- [28] A. Schönbeck, Compact squeezed-light source at 1550 nm, Ph.D. thesis, Universität Hamburg, 2018.
- [29] M. J. Yap, D. W. Gould, T. G. McRae, P. A. Altin, N. Kijbunchoo, G. L. Mansell, R. L. Ward, D. A. Shaddock, B. J. J. Slagmolen, and D. E. McClelland, Squeezed vacuum phase control at 2 μm , *Opt. Lett.* **44**, 5386 (2019).
- [30] F. Meylahn, N. Knust, and B. Willke, Stabilized laser system at 1550 nm wavelength for future gravitational-wave detectors, *Phys. Rev. D* **105**, 122004 (2022).
- [31] R. Drever, J. L. Hall, F. Kowalski, J. Hough, G. Ford, A. Munley, and H. Ward, Laser phase and frequency stabilization using an optical resonator, *Appl. Phys. B* **31**, 97 (1983).
- [32] N. Uehara, E. K. Gustafson, M. M. Fejer, and R. L. Byer, Modeling of efficient mode-matching and thermal-lensing effect on a laser-beam coupling into a mode-cleaner cavity, in *Modeling and Simulation of Higher-Power Laser Systems IV* edited by U. O. Farrukh and S. Basu (SPIE-International Society for Optical Engineering, Bellingham, WA, 1997), Vol. 2989, pp. 57–68, [10.1117/12.273681](https://doi.org/10.1117/12.273681).
- [33] Laser Components GmbH, <https://www.lasercomponents.com/de-en/product/high-quantum-efficiency-photodiodes/>, accessed on 31 May 2022.
- [34] E. Schreiber, Gravitational-wave detection beyond the quantum shot-noise limit, Ph.D. thesis, Gottfried Wilhelm Leibniz Universität Hannover, 2018.
- [35] H. Vahlbruch, S. Chelkowski, B. Hage, A. Franzen, K. Danzmann, and R. Schnabel, Coherent Control of Vacuum Squeezing in the Gravitational-Wave Detection Band, *Phys. Rev. Lett.* **97**, 011101 (2006).
- [36] T. Atkutsu *et al.* (KAGRA Collaboration), Overview of KAGRA: Detector design and construction history, *Prog. Theor. Exp. Phys.* **2021**, 05A101 (2021).
- [37] B. P. Abbott *et al.* (LIGO Scientific Collaboration and Virgo Collaboration), Exploring the sensitivity of next generation gravitational wave detectors, *Classical Quantum Gravity* **34**, 044001 (2017).